An Electrochemical Impedance Immunosensor Based on Gold Nanoparticle-Modified Electrodes for the Detection of HbA1c in Human Blood

Author:
Liu, G; Iyengar, SG; Gooding, JJ

Publication details:
Electroanalysis
v. 24
Chapter No. 7
pp. 1509 - 1516
1040-0397 (ISSN); 1521-4109 (ISSN)

Publication Date:
2012

Publisher DOI:
https://doi.org/10.1002/elan.201200233

An Electrochemical Impedance Immunosensor Based on Gold Nanoparticle-Modified Electrodes for the Detection of HbA1c in Human Blood

Guozhen Liu[a], Sridhar G. Iyengar[b], J. Justin Gooding[a*]

[a]*School of Chemistry, The University of New South Wales, Sydney, NSW 2052, Australia*

[b]*AgaMatrix, Inc. 7C Raymond Avenue Salem, NH 03079, USA*

[*]Corresponding author: Justin.gooding@unsw.edu.au

Abstract

A label-free immunosensor for the detection of HbA1c was developed based on gold nanoparticle (AuNP)-aryl diazonium salt modified glassy carbon (GC) electrode where transduction is achieved using electrochemical impedance spectroscopy (EIS). GC electrodes were first modified with 4-aminophenyl (Ph-NH_2) layers to which AuNPs were attached. Thereafter an oligo(ethylene glycol) (OEG-COOH) species were covalently attached to the remaining free amine groups on the Ph-NH_2 surface. The AuNP surfaces were further modified with Ph-NH_2 followed by attachment of a glycosylated pentapeptide (GPP), an analogon to HbA1c. Exposure of this interface to anti-HbA1c IgG resulted in a change in charge transfer resistance (R_{ct}) due to the anti-HbA1c IgG selectively complexing to the surface bound GPP. To detect the amount of HbA1c, a competitive inhibition assay was employed where the surface bound GPP and HbA1c in solution compete for the anti-HbA1c IgG antibodies. The higher the concentration of HbA1c, the less antibody binds to the sensing interface and the lower the change of R_{ct}. The response of the immunosensor is linear with the HbA1c% of total hemoglobin in the range of 0%-23.3%. This competitive inhibition assay can be used for the detection of HbA1c in human blood. The performance of the immunosensor for detection of HbA1c in human blood is comparable to the clinical lab method.

Keywords: Immunosensor; Electrochemical impedance spectroscopy; HbA1c; Gold nanoparticles

1. Introduction

The development of sensing interfaces for the sensitive, selective, and straightforward measurement of biomarker proteins in clinical samples is essential for point-of-care disease diagnosis.[1] In order to provide useful information, detection platforms must exhibit high levels of specificity, low detection limits, and robust performance in biological fluids like blood and serum. Electrochemical methods have advantages for clinical diagnosis due to the relatively low cost and the potential for miniaturization and automation.[2] A variety of high-performing protein detection platforms based on electrochemical readout are under development,[3-5] and show great promise for the development of biomarker analyzers. However, many challenges still remain regarding the development of simple analysis systems that are cost-effective and robust enough for clinical use.

HbA1c is a stable minor haemoglobin variant formed by a non-enzymatic reaction of glucose with *N*-terminal valine of an adult haemoglobin β chain. HbA1c is the main diabetes marker protein for monitoring a person's average blood sugar level over the preceding 2-3 months.[6] Due to the importance of monitoring HbA1c for tracking the effectiveness of a diabetics treatment regime, numerous analytical methods have been developed for its analysis.[7-18] Electrochemical immunoassays in particular, have been applied for the detection of HbA1c due to the high specificity of the HbA1c monoclonal antibody.[11,19-25] However, the majority of these sensing interfaces are based on boronate-affinity[10,22,24,26-29] and involve enzyme labeling process.[11,23] Such assays are reasonably complicated to perform, requiring washing and rinsing steps, and lacking of specificity to HbA1c resulting in inaccurate results when other red blood cells variants, such as haemoglobin S, are present.[30] Recently a label-free electrochemical immuno-biosensor based on a mixed layer of an oligo(phenylethynylene) molecular wire and an oligo(ethylene glycol) (OEG) component modified on glassy carbon (GC)

electrodes for the detection of HbA1c with the clinically relevant range has been developed by Liu *et al*.[31] The molecular wire/OEG sensing interface provides a quick and reliable method for the detection of HbA1c in serum without any further separation steps. However, the stability of the sensing interface is compromised by the sensitivity of the molecular wire to light and air. Thus, an alternative electrochemical immunosensor with improved stability is highly desirable.

Gold nanoparticles (AuNP) modified electrodes have good potential in electrochemical sensing because they have been shown to create conducting channels through otherwise passivated electrodes which allows the fabrication of modified electrodes with low background capacitances and well-defined sensing sites.[32-36] In essence, the AuNPs can be used to replace the molecular wire in our previous immunosensor[Liu, 2012 #254], thus providing a simple strategy to developing antifouling electrodes for electrochemical sensing. A recent study by us has reported on an impedance immunosensor based on AuNP immobilised onto an aryl diazonium salt modified electrode for the detection of anti-biotin IgG.[37] Furthermore, we have carried out further work on the development of a highly stable AuNP sensing interface in which AuNP are immobilised onto organic layers through formation of a C-Au bond instead of the more common S-Au bond or NH-Au bonds.[38]

The purpose of the present study, is to demonstrate the utility of these advances for the development of a Faradaic impedance based biosensor for the quantification of HbA1c in human blood using a unique sensing interface. Specifically the sensing interface is composed of two key components: AuNP and oligo(ethylene glycol) (OEG-COOH) molecules. The OEG-COOH species limits non-specific adsorption of proteins such that selective binding of anti-HbA1c antibodies to the AuNPs occurs. The AuNPs are modified with the epitope *N*-glycosylated pentapeptide (GPP), an analogue of the HbA1c binding site to which anti-HbA1c IgG binds with high affinity. The amount of HbA1c is determined using a competitive inhibition assay where

HbA1c in solution binds to anti-HbA1c IgG antibody in solution and any uncomplexed antibody can then selectively bind to the electrode surface to cause an increase in charge transfer resistance. Hence the more analyte present, the less anti-HbA1c IgG that bonds to the electrode surface and the smaller the increase in charge transfer resistance.

2. Experimental Section

2.1. Reagents and Materials

HbA1c control samples of four levels of glycosylated haemoglobin were obtained from Kamiya Biomedical Company (USA), and used without further purification. *N*- glycosylated pentapeptide (*N*- glycosylated-Val-is-Leu-Thr-Pro, purity by HPLC > 97.5 %) was purchased from Tocris bioscience (UK). Human HbA1c monoclonal antibody IgG (anti-HbA1c IgG) was supplied from Abnova (USA). Reagent grade dipotassium orthophosphate, potassium dihydrogenate orthophosphate, potassium chloride, sodium hydroxide, sodium chloride, sodium nitrite, hydrochloric acid, methanol, and diethyl ether were purchased from Ajax Chemicals Pty Ltd. (Sydney, Australia). Ruthenium (III) hexamine chloride ($Ru(NH_3)_6Cl_3$), 2[2-(2-methoxyethoxy)ethoxy] acetic acid (OEG-COOH), 1-ethyl-3-(3-dimethylaminopropyl) carbodiimide hydrochloride (EDC), *N*-hydroxysuccinimide (NHS), 1,3-dicyclohexylcarbodiimide (DCC), *p*-phenylenediamine, hemoglobin, bovine serum albumin (BSA), anti-pig IgG, anti-biotin IgG from goat, and absolute ethanol were obtained from Sigma-Aldrich (Sydney, Australia). All reagents were used as received, and aqueous solutions were prepared with purified water (18 MΩ cm, Millipore, Sydney, Australia). Phosphate buffered saline (PBS) solutions were 0.137 M NaCl and 0.1 M K_2HPO_4/KH_2PO_4 and adjusted with NaOH or HCl solution to pH 7.3. Phosphate buffer solutions used in this work were 0.05 M KCl and 0.05 M K_2HPO_4/KH_2PO_4 and adjusted with NaOH or HCl solution to pH 7.0.

2.2. Electrode preparation

GC electrodes were purchased as 3-mm-diameter disks from Bioanalytical Systems Inc., USA. The electrodes were polished successively with 1.0, 0.3, and 0.05 μm alumina slurries made from dry Buehler alumina and Milli-Q water on microcloth pads (Buehler, Lake Bluff, IL, USA). The electrodes were thoroughly rinsed with Milli-Q water and sonicated in Milli-Q water for 2 min after polishing. Before derivatization, the electrodes were dried under an argon gas stream.

2.3. Fabrication of AuNP modified sensing interface

As shown in Scheme 1, GC electrodes are first modified with 4-aminophenyl (Ph-NH_2) to form surface **1** by *in situ* electrochemically reductive adsorption of *p*-phenylenediamine,[39] and then the distal amine groups are partially converted to diazonium groups by incubating surface **1** in $NaNO_2$ and HCl solution to form a 4-phenyl diazonium chloride modified interface. Subsequently, scanning the potential of the modified surface between 0.5 V and -0.5 V in AuNP solution results in the electrochemical reduction of the diazonium moieties to radicals that bind to the AuNP to form a stable bond believed to be a C-Au. This is referred to as surface **2** and was reported previously.[38] It was noted by XPS that only 10% amines were converted to aryl diazonium salts indicating free amine groups remain on surface **2** (Scheme 1). Thus OEG-COOH can be attached to the amines on surface **2** through an amide bond by incubation of surface **2** in absolute ethanol solution containing 10 mM OEG-COOH and 40 mM DCC for 6 h at the room temperature to give surface **3**. Subsequently, the AuNPs on surface **3** can be further functionalized with Ph-NH_2, to allow subsequent attachment of the epitope to the AuNPs. The AuNPs are modified with the 4-aminophenyl derivative, by scanning potential between 0.5 V and -0.5 V at 0.5 M HCl solution containing 1 mM $NaNO_2$ and 1 mM *p*-phenylenediamine for two cycles at the scan rate of 100 mV s^{-1}. This surface is referred to as surface **4**. Incubation of

surface **4** in 2 mM solution of GPP in phosphate buffer pH 6.8 containing 20 mM EDC and 10 mM NHS for 4 h at 4 ^{o}C results in the covalent attachment of GPP to achieve surface **5**. Surface **5** is the sensing interface that can be used for the detection of HbA1c in human blood using a competitive inhibition assay.

Scheme 1

2.4. Preparation of HbA1c control samples

The lyophilized HbA1c control samples are a haemolysate prepared from packed human erythrocytes, with stabilizers added to maintain haemoglobin in the reduced state for the accurate calibration of the HbA1c procedure. Each lyophilized control sample was reconstituted by adding 0.5 mL Milli-Q water, and the mixture was mixed gently for 10 min and stored at 4 ^{o}C as a stock solution. The glycosylated haemoglobin levels were 4.6%, 8%, 12.4% and 15.1%, respectively, of total haemoglobin (glycosylated and non- glycosylated) concentration for each control sample. Samples with other glycosylated haemoglobin level were prepared by mixing control sample R1 (4.6%) and control sample R4 (15.1%) stock solutions with different ratio. To perform the competitive inhibition assay, samples with HbA1c analyte were preincubated with 2 μg mL^{-1} anti-HbA1c IgG for 30 min. Then 5 μL of mixture of HbA1c and anti-HbA1c IgG were applied to the working area of GPP terminated GC electrode surfaces for 5 min followed by electrochemistry measurement.

2.5. Instrumentation and procedure

All voltammetry measurements were performed with a BAS-100B electrochemical analyzer (Bioanalytical System Inc. Lafayette, IL) and a conventional three-electrode system, comprising a gold working electrode, a platinum foil as the auxiliary electrode, and an Ag/AgCl 3.0 M NaCl

electrode (from BAS) as reference. All potentials were reported *versus* the Ag/AgCl reference electrode at room temperature. The EIS measurements were performed using a Solartron SI 1287 Electrochemical Interface coupled with an SI 1260 Frequency Response Analyser (Solartron Analytical, Hampshire, England). The 1 mM $Ru(NH_3)_6^{3+}/Ru(NH_3)_6^{2+}$ redox couple in phosphate buffer solution (pH 7.0) was used as the electrolyte solution. EIS measurements were recorded with a 10 mV sinusoid superimposed on a dc potential of -0.199 V within the frequency range of 10^{-1}-10^{5} Hz and 5 points per decade of frequencies at room temperature. The Z-view software was used for complex circuit modeling. Scanning electron microscopy (SEM) was carried out using a Hitachi S-900 SEM (Berkshire, England).

X-ray photoelectron spectra were collected from GC plate (Carbon vitreous foil version 6, Goodfellow Cambridge-Limited England) on a VG EscaLab 220-IXL spectrometer with a monochromated Al Kα source (1486.6 eV), hemispherical analyzer and multichannel detector. The spectra were accumulated at a take-off angle of 90º with a 0.79 mm^2 spot size at a pressure of less than 10^{-8} mbar. The pass energy for the survey scan is 100 eV and for the narrow scan 20 eV. The step size for the survey scan is 1.0 eV and for the narrow scan 0.1 eV. Survey spectra (0-1100 eV) were obtained, followed by high resolution spectra of the C1s, O1s and N1s regions. The spectra were calibrated on the C1s Peak (285.0 eV) or on the $Au4f_{7/2}$ peak (84.0 eV). Atomic sensitivity factors are C1s 1.0, O1s 2.93, N1s 1.8, $Au4f_{7/2}$ 9.58. Spectra were analysed using XPSPEAK4.1 software. The percentage coverage for the different elements and sub-groups were estimated from the corresponding fitted areas.

3. Results and Discussion

3.1. Electrochemical characterization of AuNP modified sensing interface

The fabrication and electrochemical characterization of surface **2** have been reported previously.[38] GC surfaces are first modified with Ph-NH_2 by *in situ* aryl diazoniums salt chemistry followed by conversion of amines to diazonium species. Then the electrochemistry of the surface diazonium species in AuNP solution results in the attachment of AuNP to form a stable bond, presumable an Au-C bond, to the AuNPs to give surface **2**. XPS results indicate there are still free amine groups on surface **2**.[38] Thus OEG-COOH can be covalently attached to surface **2** via the formation of an amide bond by incubation of surface **2** in ethanol solution containing OEG-COOH and DCC for 3 h to obtain surface **3** (Scheme 1). The characterization of the formation of the sensing interface by electrochemistry and X-ray photoelectron spectroscopy is discussed in detail in the supplementary information (see Fig. SI 1-3).

3.2. AuNP distribution on the sensing interface by SEM

SEM was used to characterize the final sensing interface (surface **5**). Based on the SEM images, the size of AuNP was about 10±2 nm (n=500, 95% confidence), and these AuNP were randomly distributed. There was no discernable difference between SEM images for surface **2**, surface **3**, surface **4**, and surface **5** (Fig. 1).

Fig. 1

3.3. EIS characterisation of the sensing interface

Figure 2 shows impedance results for the fabricated surfaces in the presence of $Ru(NH_3)_6^{3+}/Ru(NH_3)_6^{2+}$ redox couple in phosphate buffer solution. A significant change in the diameter of the semicircle in the Nyquist plot (Fig. 2 a),[40] and hence the charge transfer resistance (R_{ct}), was observed with the stepwise fabrication of the interface. After the fabrication of Ph-NH_2 film, the R_{ct} was increased significantly due to the organic layer hindering the ability

of the redox molecule from accessing the electrode. However, upon attachment of AuNP there is a dramatic decrease in the R_{ct}, consistent with other studies of AuNP on organic layers where nanoparticles can "switch on" Faradaic electrochemistry at an otherwise blocking layers.[33,41] Attachment of the OEG molecules, sees an increase in R_{ct}, but not as high as observed before the AuNPs were coupled to the interface. A further increase in R_{ct} were also observed after the subsequence attachment of Ph-NH_2, and then GPP, to give the sensing interface, surface **5**. As can be seen from the Bode plot (Fig 2 b), there are much larger increases in impedance at the lower frequencies. Therefore changes in impedance at lower frequencies could be used for sensing the interfacial properties of the prepared immunosensor.

Fig. 2

A Randles circuit (Fig. 2 c inset) is used to fit the Nyquist plot. This Randles circuit includes the solution resistance (R_s), R_{ct}, the double layer capacitance was treated as a constant phase element impedance (CPE) indicating the depressed semi-circle obtained, and the Warburg impedance element (Z_W) which is the consequence of the ions diffusion from the bulk of the electrolyte to the electrode interface. Ideally, Z_W and R_s represented the bulk properties of the electrolyte solution and diffusion features of the redox probe in solution and, thus, are not affected by modifications occurring on the electrode surface.[42] On the other hand, CPE and R_{ct} are related to the dielectric and insulating features at the electrode/electrolyte interface, hence they are affected by the changes at the electrode surface. The capacitance changes are not as sensitive as the electron transfer resistance. Surface **5**, is the surface that is used for sensing. Incubating this surface in a solution of 500 ng mL^{-1} anti-HbA1c IgG results in a larger increase in R_{ct} than any of the other modifications. This large R_{ct} is encouraging as this increase in R_{ct} will be used as the analytical signal. Fig. 2 c shows the experimental (solid line) and the fitted (scattered line) Nyquist plot of the GPP modified sensing interface after exposure to the mixture of 2 μg mL^{-1}

anti-HbA1c IgG and 12% HbA1c. There is a good fitting over the entire measurement frequency range.

The results of the experimental data fitting using the equivalent circuit are summarized in Table 1. It is noted that a negligible change in R_s was observed during the stepwise modification process. Taking into account the effect of the roughness of electrode surfaces, CPE can be expressed as CPE= $(A\omega)^{-\alpha}$ where A is a proportionality factor, ω □is the angular frequency, and α is an exponential term with a value between 0 and 1. When α is 1, the constant phase element translates to an ideal capacitor. The deviation of α from unity was attributed to the homogeneities of analyzed layer, such as roughness or defects.[43-44] As shown in Table 1, all these values are close to 0.85, indicating there are minimal defects in the modification layer on the interfaces. The changes in R_{ct} were much larger than those in other impedance components. Thus, R_{ct} is a suitable signal for sensing the interfacial properties of the prepared immunosensor during all these assembly procedures.

Table 1

3.4. Selectivity of the sensing interface

To study the selectivity, the sensing interface was exposed to various concentrations of anti-HbA1c IgG which has high affinity with GPP, and anti-pig IgG as an antibody which has no affinity with GPP. After the incubation of surface **5** with anti-HbA1c IgG, R_{ct} increased because binding of the protein to the sensing interface decreased access of the $Ru(NH_3)_6^{3+}/Ru(NH_3)_6^{2+}$ redox couple to the AuNP on the modified surface. In order to compare the different performance of electrodes in equivalent conditions, the relative values ($R_{ct(i)}$-$R_{ct(o)}/R_{ct(0)}$) were used. $R_{ct(o)}$ and $R_{ct(i)}$ are respectively the charge transfer resistance of surface **5** before and after reaction with antibodies. Fig. 3 shows plots that correspond to the resistance change (R_{ct}) with

different concentrations of the anti-HbA1c IgG, anti-biotin IgG, and anti-pig IgG. A linear relationship between the electron transfer resistance and anti-HbA1c IgG concentration was found ranging from 1-500 ng mL^{-1} with the detection limit of 1 ng mL^{-1}. When the concentration of antibody was increased to 500 ng mL^{-1}, the change of normalized charge transfer resistance gradually leveled out, indicating that all the available binding sites on the gold nanoparticles were occupied with the anti-HbA1c IgG. Note that over the concentration range of anti-HbA1c IgG in Fig. 3 the R_{ct} increased six fold. Thus, the fabricated sensing interfaces (surface **5**) can be used for detection of anti-HbA1c IgG. However, there is almost no change in the impedance with the increase of concentration of anti-biotin IgG or anti-pig IgG indicating the sensing interface is not sensitive to the non-specific antibody such as anti-biotin IgG or anti-pig IgG. In addition, incubation of the sensing interface with 1 μg mL^{-1} BSA, as a different protein from IgG, for 3 h at room temperature did not show significant variation of R_{ct}. These results further indicate the sensing interface can resist the non-specific adsorption of protein due to the presence of OEG molecules.[45] With the ability to resist non-specific protein adsorption, the modified sensing interface has good selectivity and can be used as the immunosensor for the detection of anti-HbA1c IgG.

Fig. 3

3.5. Calibration curve for the detection of HbA1c in serum

Surface **5** was used as the sensing interface for detection of HbA1c in serum with different concentrations. The mechanism of the fabricated EIS immunosensor (Scheme 1) for the detection of HbA1c is based on a competitive inhibition assay. In a competitive inhibition assay the analyte, HbA1c, and the antibodies (anti-HbA1c IgG) are both in solution. Any antibody that is uncomplexed can then bind to the surface bound GPP and cause a change in R_{ct}. Hence the

higher the concentration of HbA1c, the lower the amount of anti-HbA1c that is free to bind to the interface and hence the lower the measured R_{ct}. Fig. 4 a shows the derived calibration plot that corresponds to the electron transfer resistance at the sensing interface with different concentration of HbA1c. A linear relationship between the change of electron transfer resistance and HbA1c% of total hemoglobin (R^2=0.97) was observed between the extremes of concentrations tested of 4.6% and 23.3% HbA1c to total haemoglobin which covers the clinically relevant range of between 5% and 20%. In order to test the long-time stability of the sensing interface, sensors modified to give surface **5** were incubated in PBS solution for different periods time at 4 °C. Subsequently the R_{ct} was measured after incubation in 250 ng mL^{-1} anti-HbA1c IgG (Fig. 4 b). There is no obvious deteriorating in sensor performance even after 40 days of sensor storage at 4 °C (the standard deviation is between 7% and 15% for three parallel measurements at each testing day).

Fig. 4

3.6. Application of the immunosensor in human blood

The above results have demonstrated that the fabricated EIS immunosensor exhibits good selectivity, sensitivity, and stability for the detection of HbA1c in serum. The performance of this fabricated EIS immunosensor was also assessed for the detection of HbA1c in a real sample and was compared with an independently measured value by different operators using the clinical method used at the Douglass Hanly Moir Pathology, Sydney. A human blood sample donated from the healthy adult was collected. The content of HbA1c of a neat blood sample (i.e. no dilution) applied directly to the sensing electrode was determined to be 4.88%±1.04% (n=3, 95% confidence) by the EIS immunosensor. The clinical method gave a similar value of 5.80%. Note the standard deviation for measurements of this type using a standard operating procedure

are typically 0.1 for HbA1c levels around 5.5%[, #255]. Although not completely concordant, the two values are reasonably similar considering no sample preparation being performed on the sample measured by the immunosensor other than a freezing step to release the HbA1c from the cells. The closeness of these two measurements illustrates that the antifouling layer is effective at allowing the electrochemical immunosensor to operate in complex samples such as blood. We believe that this preliminary result in principle shows that the EIS immunosensor could be used for point-of-care diagnosis of HbA1c levels for evaluation of diabetes.

4. Conclusions

A stable label-free immunosensor for the detection of HbA1c was developed based on AuNP-diazonium salt modified GC electrodes by using the EIS technique. The modified sensing interface (surface **5**) is fabricated by the stepwise covalent attachment. Due to the affinity between epitope GPP and HbA1c monoclonal antibody, the fabricated sensing interface can be used for detection of anti-HbA1c IgG with the detection limit of 1 ng mL^{-1}. Most importantly, the modified sensing interface demonstrates high stability and selectivity and can be used for the detection of HbA1c through a competitive inhibition assay. It is observed that there is a good linear relationship between the change of charge transfer resistance R_{ct} and the concentration of HbA1c. The developed EIS immunosensor can be used for the detection of HbA1c in human blood, and the result is comparable to that obtained by clinical method. The present sensing methodology represents a very attraction alternative to the existing method for the detection of HbA1c in serum with high stability, sensitivity, selectivity, and simple instrumentation, and is suitable for use at point-of-care diagnosis of diabetes.

5. Acknowledgements

The authors gratefully thank Dr Erwann Luais for technical assistance on running XPS. Aspects of this work were supported financially by the Australia Research Council Linkage (LP100200593).

7. References

[1] N. L. Rosi, C. A. Mirkin, *Chem. Rev.* **2005**, *105*, 1547.

[2] J. Wang, *J. Pharm. Biomed. Anal.* **1999**, *19*, 47.

[3] J. Das, S. O. Kelley, *Anal. Chem.* **2011**, *83*, 1167.

[4] M. H. Yang, A. Javadi, H. Li, S. Q. Gong, *Biosens. Bioelectron.* **2010**, *26*, 560.

[5] V. Mani, B. V. Chikkaveeraiah, V. Patel, J. S. Gutkind, J. F. Rusling, *ACS Nano* **2009**, *3*, 585.

[6] The diabetes control and complications trial research group, *N. Engl. J. Med.* **1993**, *329*, 977.

[7] M. B. D. Guntinas, R. Wissiack, G. Bordin, A. R. Rodriguez, *J. Chromatogr. B-Anal. Tech. Biomed. Life Sci.* **2003**, *791*, 73.

[8] J. D. Lafferty, A. G. McFarlane, D. H. K. Chui, *Arch. Pathol. Lab. Med.* **2002**, *126*, 1494.

[9] Y. C. Li, J. O. Jeppsson, M. Jornten-Karlsson, E. L. Larsson, H. Jungvid, I. Y. Galaev, B. Mattiasson, *J. Chromatogr. B-Anal. Tech. Biomed. Life Sci.* **2002**, *776*, 149.

[10] J. Pribyl, P. Skladal, *Anal. Chim. Acta* **2005**, *530*, 75.

[11] T. Tanaka, S. Tsukube, K. Izawa, M. Okochi, T. K. Lim, S. Watanabe, M. Harada, T. Matsunaga, *Biosens. Bioelectron.* **2007**, *22*, 2051.

[12] L. Menard, M. E. Dempsey, L. A. Blankstein, H. Aleyassine, M. Wacks, J. S. Soeldner, *Clin. Chem.* **1980**, *26*, 1598.

[13] J. M. Burrin, R. Worth, L. A. Ashworth, S. Currie, K. G. M. M. Alberti, *Clin. Chim. Acta* **1980**, *106*, 45.

[14] N. Wangoo, J. Kaushal, K. K. Bhasin, S. K. Mehta, C. R. Suri, *Chem. Commun.* **2010**, *46*, 5755.

[15] O. S. Zhernovaya, V. V. Tuchin, I. V. Meglinski, *Laser Phys. Lett.* **2008**, *5*, 460.

[16] K. Hirokawa, K. Nakamura, N. Kajiyama, *FEMS Microbiol. Lett.* **2004**, *235*, 157.

[17] K. P. Peterson, J. G. Pavlovich, D. Goldstein, R. Little, J. England, C. M. Peterson, *Clin. Chem.* **1998**, *44*, 1951.

[18] M. S. Kiran, T. Itoh, K. I. Yoshida, N. Kawashima, V. Biju, M. Ishikawa, *Anal. Chem.* **2010**, *82*, 1342.

[19] M. Okochi, H. Ohta, T. Tanaka, T. Matsunaga, *Biotech. Bioengi.* **2005**, *90*, 14.

[20] T. Tanaka, T. Matsunaga, *Biosens. Bioelectron.* **2001**, *16*, 1089.

[21] L. M. Thienpont, K. Van uytfanghe, A. P. De Leenheer, *Clin. Chim. Acta* **2002**, *323*, 73.

[22] S. Q. Liu, U. Wollenberger, M. Katterle, F. W. Scheller, *Sens. Actuat. B-Chem.* **2006**, *113*, 623.

[23] D. Stollner, W. Stocklein, F. Scheller, A. Warsinke, *Anal. Chim. Acta* **2002**, *470*, 111.

[24] J. Halamek, U. Wollenberger, W. Stocklein, F. W. Scheller, *Electrochim. Acta* **2007**, *53*, 1127.

[25] J. Halamek, U. Wollenberger, W. F. M. Stocklein, A. Warsinke, F. W. Scheller, *Anal. Lett.* **2007**, *40*, 1434.

[26] H. B. Chandalia, P. R. Krishnaswamy, *Curr. Sci.* **2002**, *83*, 1522.

[27] J. Pribyl, P. Skladal, *Biosens. Bioelectron.* **2006**, *21*, 1952.

[28] J. T. Liu, L. Y. Chen, M. C. Shih, Y. Chang, W. Y. Chen, *Anal. Biochem.* **2008**, *375*, 90.

[29] J. Y. Park, B. Y. Chang, H. Nam, S. M. Park, *Anal. Chem.* **2008**, *80*, 8035.

[30] L. K. Koskinen, *Clin. Chim. Acta* **1996**, *253*, 159.

[31] G. Z. Liu, S. M. Khor, S. G. Iyengar, J. J. Gooding, *Analyst* **2012**, *137*, 829.

[32] J. Dyne, Y. S. Lin, L. M. H. Lai, J. Z. Ginges, E. Luais, J. R. Peterson, I. Y. Goon, R. Amal, J. J. Gooding, *Chemphyschem* **2010**, *11*, 2807.

[33] J. B. Shein, L. M. H. Lai, P. K. Eggers, M. N. Paddon-Row, J. J. Gooding, *Langmuir* **2009**, *25*, 11121.

[34] C. R. Bradbury, J. J. Zhao, D. J. Fermin, *J. Phys. Chem. C* **2008**, *112*, 10153.

[35] J. J. Zhao, C. R. Bradbury, D. J. Fermin, *J. Phys. Chem. C* **2008**, *112*, 6832.

[36] G. Le Saux, S. Ciampi, K. Gaus, J. J. Gooding, *ACS Appl. Mater. Interf.* **2009**, *1*, 2477.

[37] G. Z. Liu, J. Q. Liu, T. P. Davis, J. J. Gooding, *Biosens. Bioelectron.* **2011**, *26*, 3660.

[38] G. Z. Liu, E. Luais, J. J. Gooding, *Langmuir* **2011**, *27*, 4176.

[39] G. Z. Liu, M. Chockalingham, S. M. Khor, A. L. Gui, J. J. Gooding, *Electroanalysis* **2010**, *22*, 918.

[40] F. Darain, D. S. Park, J. S. Park, Y. B. Shim, *Biosens. Bioelectron.* **2004**, *19*, 1245.

[41] S. L. Horswell, I. A. O'Neil, D. J. Schiffrin, *J. Phys. Chem. B* **2003**, *107*, 4844.

[42] A. E. Radi, X. Munoz-Berbel, M. Cortina-Puig, J. L. Marty, *Electrochim. Acta* **2009**, *54*, 2180.

[43] E. Barsoukou, J. R. MacDonald *Impedance spectroscopy: theory, experiment, and applications*; Wiley Interscience: New Jersey, 2005.

[44] H. Hillebrandt, G. Wiegand, M. Tanaka, E. Sackmann, *Langmuir* **1999**, *15*, 8451.

[45] S. M. Khor, G. Liu, C. Fairman, S. G. Iyengar, J. J. Gooding, *Biosens. Bioelectron.* **2011**, *26*, 2038.

Captions:

Fig. 1. SEM image for surface **5** at 300 K magnification.

Fig. 2. (a) Nyquist plot and (b) Bode plot, for difference surfaces in the presence of $Ru(NH_3)_6^{3+}/Ru(NH_3)_6^{2+}$ redox couple in phosphate buffer solution; (c) the experimental (solid line) and the fitted (scattered points) Nyquist plot of surface 5 after exposure to the mixture of 2 μ g mL^{-1} anti-HbA1c IgG and 12% HbA1c. Inset: the Randles equivalent circuit for the impedance spectroscopy measurement.

Fig. 3. The impedance change of surface **5** sensing interface with the concentration of target anti-HbA1c IgG (triangle dot), anti-biotin antibody (square dot), and anti-pig IgG (circle dot).

Fig. 4. (a) The calibration plot corresponding to the change of electron transfer resistance of the immunosensor with the concentration of HbA1c; (b) the plot between the impedance response of surface **5** to 250 ng mL^{-1} target anti-HbA1c IgG and the incubation time of surface **5** in PBS at 4 °C.

Scheme 1. The schematic of fabrication of EIS immunosensor based on AuNP-diazonium salt modified sensing interface for the detection of HbA1c.

Table 1. Values of the equivalent circuit parameters of the fitting curves for the stepwise fabrication of the immunosensor interface by Z-view software.

Fig. 1

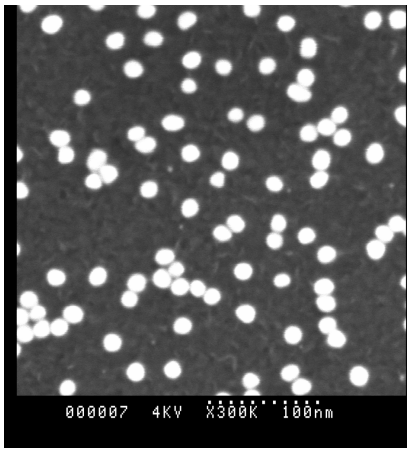

Fig. 2

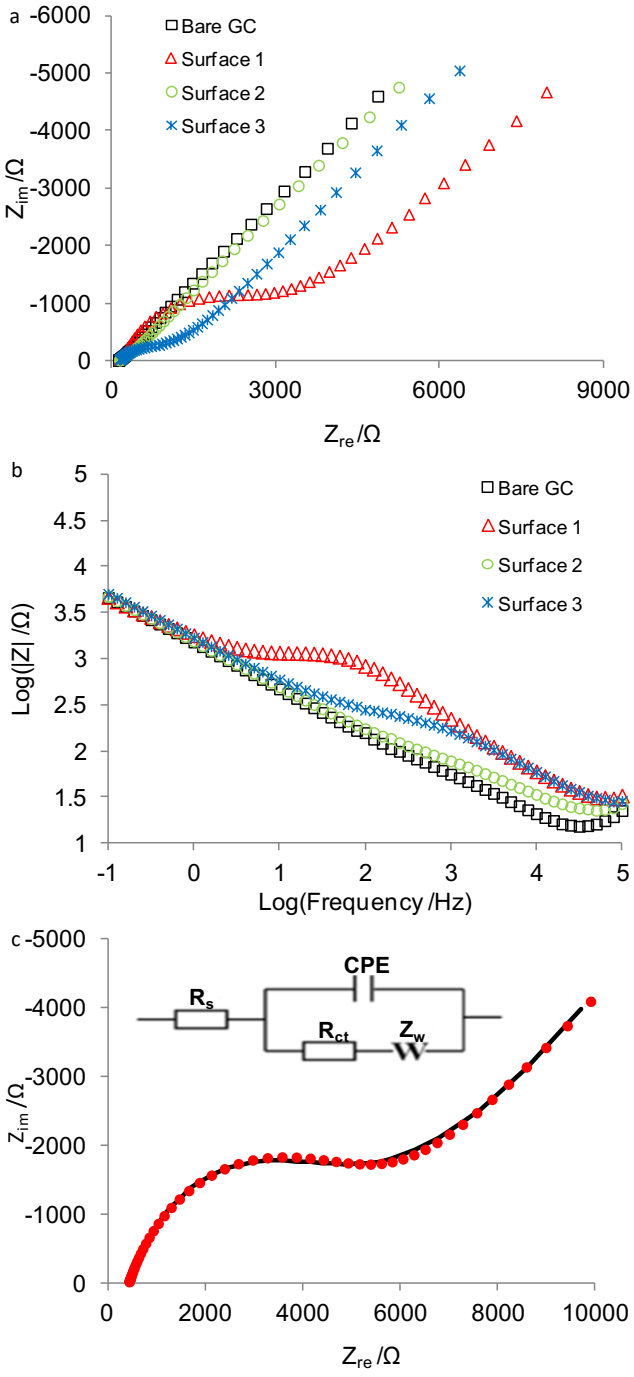
a
Bare GC
Surface 1
Surface 2
Surface 3
Z_{im}/Ω
Z_{re}/Ω
b
Bare GC
Surface 1
Surface 2
Surface 3
Log(|Z| /Ω)
Log(Frequency /Hz)
c
CPE
R_s
R_{ct}
Z_w
Z_{im} /Ω
Z_{re} /Ω

Fig. 3

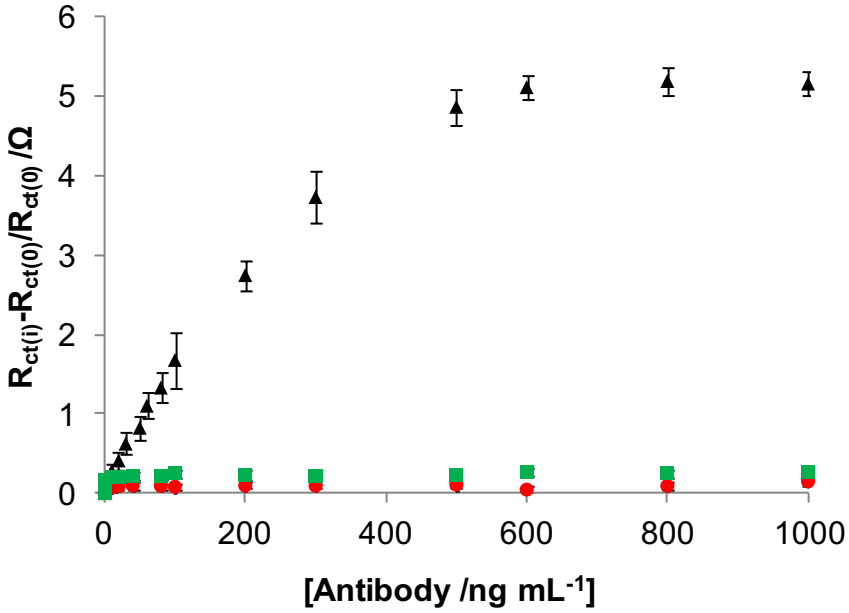
6
5
4
3
2
1
0
0
200
400
600
800
1000
$R_{ct(i)}$-$R_{ct(0)}$/$R_{ct(0)}$ /Ω
[Antibody /ng mL^{-1}]

Fig. 4

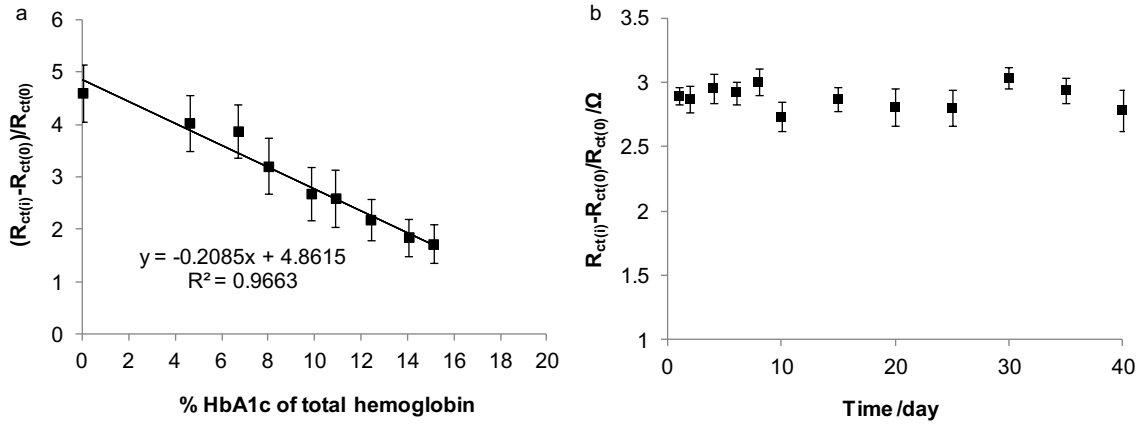
a
$(R_{ct(i)}-R_{ct(0)})/R_{ct(0)}$
y = -0.2085x + 4.8615
R² = 0.9663
% HbA1c of total hemoglobin
b
$R_{ct(i)}-R_{ct(0)}/R_{ct(0)}$ /Ω
Time /day

Scheme 1

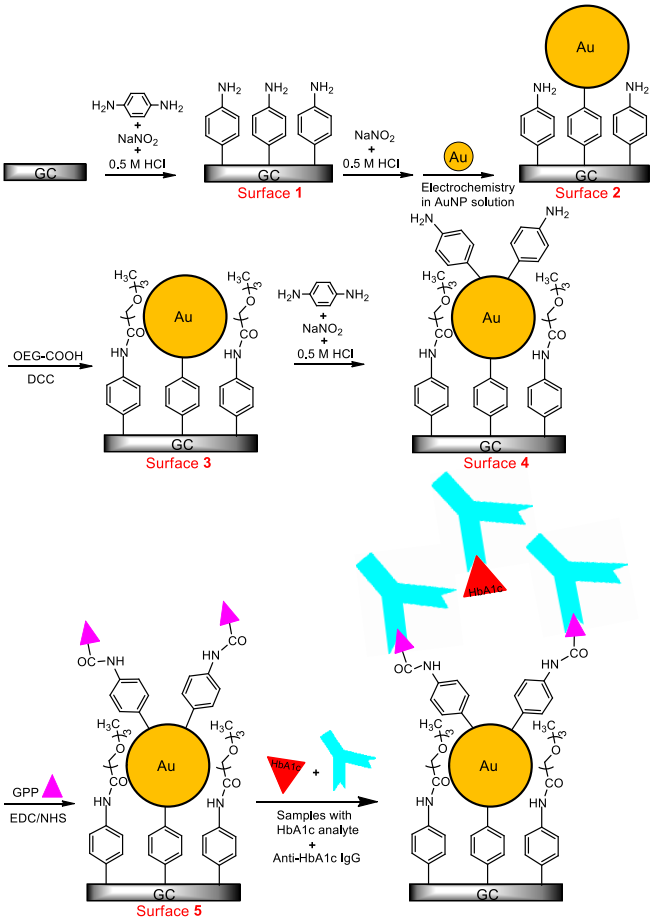
GC
0.5 M HCl
Surface 1
Au
Electrochemistry in AuNP solution
Surface 2
OEG-COOH
DCC
Surface 3
Surface 4
GPP
EDC/NHS
Surface 5
HbA1c
Samples with HbA1c analyte
Anti-HbA1c IgG

Table 1

Electrodes	R_s(Ω) (n=3, 95% confidence)	R_{ct} (Ω) (n=3, 95% confidence)	CPE($\times 10^{-6}$F) (n=3, 95% confidence)	α (n=3, 95% confidence)
Bare GC	122.4±10.7	26.9±5.2	0.69±0.21	0.85±0.02
Surface **1**	134.5±9.2	3178±86.9	2.98±0.11	0.84±0.02
Surface **2**	141.1±7.6	98.1±21.3	2.35±0.23	0.83±0.01
Surface **3**	142.0±6.8	654.3±51.6	2.98±0.09	0.82±0.01
Surface **4**	143.5±7.4	925.9±41.8	2.76±0.17	0.81±0.01
Surface **5**	125.4±13.3	1523±71.5	3.02±0.08	0.81±0.01
Exposure surface **5** to mixture of 2 μg mL^{-1} anti-HbA1c IgG and 12% HbA1c	121.9±14.0	5872±123.9	3.13±0.05	0.81±0.02